

Non-equilibrium interfaces in colloidal fluids

Markus Bier* and Daniel Arnold

*Max-Planck-Institut für Intelligente Systeme, Heisenbergstr. 3,
70569 Stuttgart, Germany, and Institut für Theoretische Physik IV,
Universität Stuttgart, Pfaffenwaldring 57, 70569 Stuttgart, Germany*

(Dated: 11 September 2013)

The time-dependent structure, interfacial tension, and evaporation of an oversaturated colloid-rich (liquid) phase in contact with an undersaturated colloid-poor (vapor) phase of a colloidal dispersion is investigated theoretically during the early-stage relaxation, where the interface is relaxing towards a local equilibrium state while the bulk phases are still out of equilibrium. Since systems of this type exhibit a clear separation of colloidal and solvent relaxation time scales with typical times of interfacial tension measurements in between, they can be expected to be suitable for analogous experimental studies, too. The major finding is that, irrespective of how much the bulk phases differ from two-phase coexistence, the interfacial structure and the interfacial tension approach those at two-phase coexistence during the early-stage relaxation process. This is a surprising observation since it implies that the relaxation towards global equilibrium of the interface is not following but preceding that of the bulk phases. Scaling forms for the local chemical potential, the flux, and the dissipation rate exhibit qualitatively different leading order contributions depending on whether an equilibrium or a non-equilibrium system is considered. The degree of non-equilibrium between the bulk phases is found to not influence the qualitative relaxation behavior (i.e., the values of power-law exponents), but to determine the quantitative deviation of the observed quantities from their values at two-phase coexistence. Whereas the underlying dynamics differs between colloidal and molecular fluids, the behavior of quantities such as the interfacial tension approaching the equilibrium values during the early-stage relaxation process, during which non-equilibrium conditions of the bulk phases are not changed, can be expected to occur for both types of systems.

I. INTRODUCTION

Interfaces between two fluid phases are commonly characterized by the interfacial tension, because this quantity is sensitive to the interfacial structure [1, 2] and, at the same time, it is easy to measure by means of numerous experimental methods developed during the last two centuries [3]. Whereas the interfacial tension is thermodynamically defined only for two-phase coexistence [2], it is frequently discussed also for non-equilibrium conditions, e.g., in the context of the adsorption dynamics of surfactants [4, 5]. Since interfaces typically extend over a spatial range of the order of the bulk correlation length, whereas the bulk phases are typically of macroscopic extension, one can intuitively expect the existence of a time scale τ^\times such that at times $t \ll \tau^\times$ the interface relaxes towards *some* local equilibrium state the properties of which are governed by the adjacent non-equilibrium bulk phases and at times $t \gg \tau^\times$ the bulk phases relax towards the global equilibrium state. In the following the processes taking place at times $t < \tau^\times$ or $t > \tau^\times$ are referred to as the “early-stage” or the “late-stage” relaxation, respectively. The late-stage relaxation processes have been extensively studied in the past, probably because here one can expect the notion of a non-equilibrium interfacial tension being applicable [6–10]. However, neither the early-stage relaxation process of the interface nor the nature of the local equilibrium state of the inter-

face in between two slowly relaxing non-equilibrium bulk phases are understood so far. Obviously, at late times, when the ultimate global equilibrium state is reached, the interfacial structure is that in between two bulk phases at coexistence. However, for non-equilibrium bulk phases it cannot even be expected a priori that the interface which has been equilibrated locally during the early-stage relaxation bears a resemblance to any structure found at global equilibrium. Moreover, one has to reckon with a non-trivial dependence of the local equilibrium interfacial structure on the properties of the adjacent non-equilibrium bulk phases. In the present work we analyze these open questions on the early-stage relaxation process.

From the experimental perspective it is difficult to study the time-dependence of the interfacial tension during the early-stage relaxation process of an interface in a molecular fluid, because it relaxes on time scales much shorter than the time of measurements of the interfacial tension. One possible solution is to consider molecular fluids close to a critical point [9] or a wetting transition [7, 8], which, however, is technically demanding due to the requirement of a stable temperature control. Here it is proposed to alternatively study the time-dependence of the interfacial tension by means of colloidal fluids which can phase-separate into a colloid-rich (liquid) phase and a colloid-poor (vapor) phase [11]. The interfacial tension in colloidal fluids is typically some orders of magnitude smaller than in molecular fluids and the relaxation times can be of the order of hours [11]. The clear separation of time scales in long relaxation times of the colloidal structure, intermediate times to measure the in-

*Electronic address: bier@is.mpg.de

terfacial tension, and short relaxation times of the solvent leads to a proper account of a time-dependent interfacial tension for colloidal fluids. For such systems the time-dependent sedimentation and interface formation in the gravitational field [11] as well as the interface fluctuation dynamics [12] have been recorded using direct microscopy imaging. However, these studies were devoted to the interface formation driven by an external field.

In the present theoretical investigation we study the early-stage formation of an interface between an oversaturated colloidal liquid in contact with an undersaturated colloidal vapor in the absence of external fields. The analogous situation in a molecular fluid would lead to the evaporation of the liquid; hence, the same term is used for colloidal fluids here. It should be stressed, that, although the colloids are dispersed in a molecular solvent, the latter is assumed to be uniformly distributed throughout the system, whereas the interface is formed by the contact of the colloid-rich and the colloid-poor phases. Here only times longer than the relaxation time of the molecular solvent are considered, for which the colloidal particles are in local equilibrium with the solvent and exhibit diffusive Brownian dynamics. An appropriate theoretical approach for this situation is dynamic density functional theory (DDFT) [13–16], which describes the conserved dynamics of time-dependent number density profiles of colloidal particles [17, 18]. Processes occurring on time scales shorter than the relaxation time of the molecular solvent, e.g., in the ballistic regime, are not considered in the following. The model of colloidal fluids used here, the formalism of DDFT, and the relevant observables, in particular the interfacial tension, are introduced in Sec. II. The results on the interfacial structure dynamics, the time-dependence of the interfacial tension, the energy dissipation during the interface formation as well as on the evaporation rates are discussed in Sec. III. Conclusions and a summary are given in Sec. IV.

II. FORMALISM

A. Model

Consider a three-dimensional dispersion of colloidal hard spheres of diameter d which in addition interact via the square-well potential

$$U(r) = \begin{cases} -\varepsilon & , r \leq \lambda \\ 0 & , r > \lambda \end{cases} \quad (1)$$

with the cohesive energy $\varepsilon > 0$ and the extension λ of the attractive well.

In the following the focus is on collective properties of the colloidal fluid which can be expressed in terms of the local number density $\varrho(\mathbf{r})$ at position \mathbf{r} . However, instead of describing the fluid structure by the number density $\varrho(\mathbf{r})$ it is more convenient to use the dimensionless occupancy $\phi(\mathbf{r}) := \varrho(\mathbf{r})/\varrho_{\max} \in [0, 1]$, where ϱ_{\max} is the

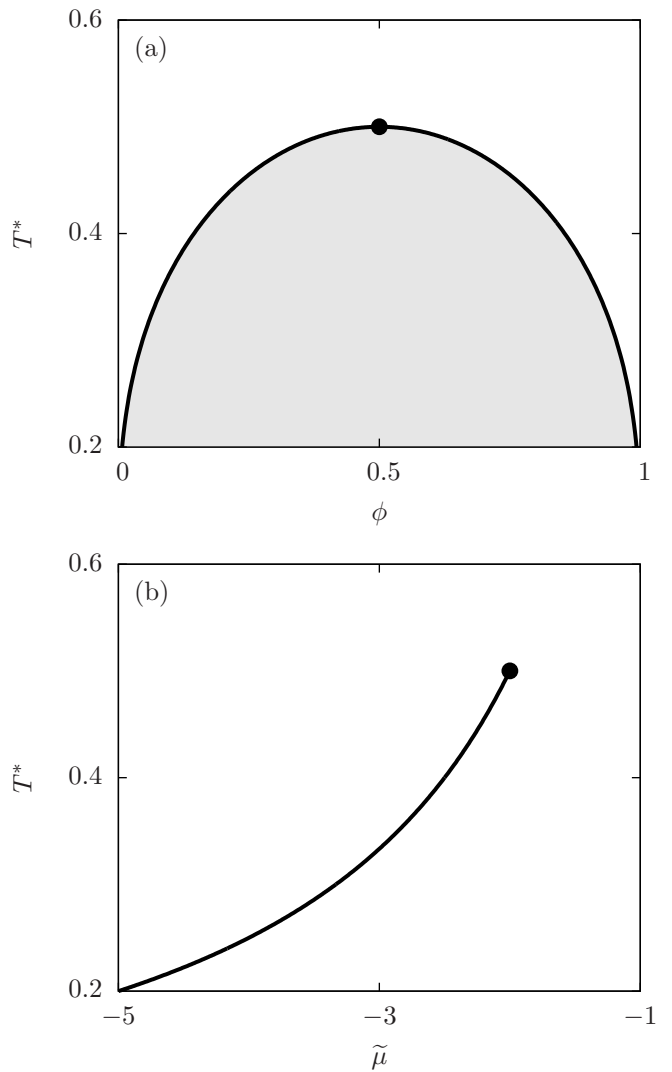


FIG. 1: Phase diagram of the colloidal fluid described in Subsec. II A of hard spheres interacting by an additional square-well potential. The solid lines represent the liquid-vapor coexistence curves $T_b^*(\phi)$ (a, see Eq. (10)) and $\tilde{\mu}_{co}(T^*)$ (b, see Eq. (8)). The two-phase coexistence region terminates in a critical point (\bullet , see Eq. (9)).

maximal number density of the fluid phase at the given temperature.

Local equilibrium is assumed in the following, since only times longer than the relaxation time of the molecular solvent are considered. Consequently the temporal evolution of the system is described in terms of a Helmholtz free energy density functional $F[\phi]$. The present study does not aim for a quantitative description of a real colloidal fluid but for a qualitative and generic account of the early-stage interface formation. Hence, in order to minimize the technical efforts, a free energy density functional

$$F[\phi] = F_{\text{HS}}[\phi] + F^{\text{ex}}[\phi] \quad (2)$$

in the spirit of Ebner, Saam, and Stroud [19] is chosen,

which comprises a *local* free energy density functional $F_{\text{HS}}[\phi]$ describing a hard-sphere fluid and a *quadratic* excess free energy functional $F^{\text{ex}}[\phi]$ to account for the square-well potential $U(r)$ (see Eq. (1)). Using a local functional $F_{\text{HS}}[\phi]$ to describe hard spheres is obviously not expected to be quantitatively precise, in particular in the context of steep interfaces, and there are numerous highly sophisticated density functionals which reproduce the structure of hard-sphere fluids well [20–22]. However, this is not expected to influence the general conclusions of this investigation, because $F_{\text{HS}}[\phi]$ leads to qualitatively correct profiles.

Here we chose the lattice-gas-like local hard-sphere functional

$$F_{\text{HS}}[\phi] = k_B T \varrho_{\text{max}} \int d^3 r [\phi(\mathbf{r}) \ln(\phi(\mathbf{r})) + (1 - \phi(\mathbf{r})) \ln(1 - \phi(\mathbf{r}))] \quad (3)$$

and the excess functional within random phase approximation (RPA)

$$F^{\text{ex}}[\phi] = \frac{\varrho_{\text{max}}^2}{2} \int d^3 r \int d^3 r' U(|\mathbf{r} - \mathbf{r}'|) \phi(\mathbf{r}) \phi(\mathbf{r}'). \quad (4)$$

The former is used, because it is the simplest form which leads to fluid densities $\varrho(\mathbf{r})$ strictly in the interval $[0, \varrho_{\text{max}}]$. Moreover, the theoretical phase diagram resulting from Eqs. (2)–(4) (see Fig. 1 and Subsec. II B) can be calculated analytically, and it agrees semi-quantitatively with the fluid parts of the phase diagrams of real colloidal dispersions [23]. The perfect symmetry of the lattice-gas model with respect to an exchange of particle and vacancy is irrelevant in the present study.

B. Phase behavior

Assuming a uniform bulk state the phase behavior of the colloidal fluid introduced in the previous Subsec. II A can be inferred from the Helmholtz free energy density

$$f = \frac{F}{V} = k_B T \varrho_{\text{max}} \left(\phi \ln(\phi) + (1 - \phi) \ln(1 - \phi) - \frac{\phi^2}{T^*} \right) \quad (5)$$

with the effective temperature

$$T^* = \left(-\frac{\varrho_{\text{max}}}{2k_B T} \int d^3 r U(|\mathbf{r}|) \right)^{-1} = \frac{3k_B T}{2\pi\epsilon\varrho_{\text{max}}\lambda^3}. \quad (6)$$

The equation of state reads

$$\frac{p}{k_B T \varrho_{\text{max}}} = -\ln(1 - \phi) - \frac{\phi^2}{T^*} \quad (7)$$

and the liquid phase coexists with the vapor phase at chemical potential

$$\tilde{\mu}_{\text{co}}(T^*) := \frac{\mu_{\text{co}}(T^*)}{k_B T} = \frac{\partial}{\partial \phi} \frac{f}{k_B T \varrho_{\text{max}}} \Big|_{\text{co}} = -\frac{1}{T^*} \quad (8)$$

below the critical point ($T^* < T_c^*$), which is located at

$$T_c^* = \frac{1}{2}, \quad \phi_c = \frac{1}{2}, \quad \tilde{\mu}_c = \tilde{\mu}_{\text{co}}(T_c^*) = -2. \quad (9)$$

Finally the liquid-vapor binodal curve is given by

$$T_b^*(\phi) = \frac{2\phi - 1}{\ln\left(\frac{\phi}{1 - \phi}\right)}. \quad (10)$$

The phase diagram is displayed in Fig. 1. Due to the choice of a simple lattice-gas-like description the phase diagram in Fig. 1(a) is symmetric with respect to the critical occupancy $\phi = \phi_c$. However, this symmetry is irrelevant to all conclusions to be drawn later.

C. Dynamic density functional theory

If the system is prepared in an arbitrary initial state $\phi(\mathbf{r}, t = 0)$, its state $\phi(\mathbf{r}, t > 0)$ evolves with time t such that the Helmholtz free energy $F[\phi(t)]$ reaches a minimum at $t \rightarrow \infty$. In the present work the colloidal processes to be described in terms of $\phi(\mathbf{r}, t)$ are much slower than the molecular degrees of freedom. Hence one can assume local thermodynamic equilibrium and define the local chemical potential [18]

$$\mu(\mathbf{r}, [\phi(t)]) = \frac{1}{\varrho_{\text{max}}} \frac{\delta F}{\delta \phi(\mathbf{r})}[\phi(t)], \quad (11)$$

which leads to a local force $-\nabla\mu(\mathbf{r}, [\phi(t)])$ that generates a flux [18]

$$\mathbf{j}(\mathbf{r}, [\phi(t)]) = -\frac{D\varrho_{\text{max}}}{k_B T} \phi(\mathbf{r}, t) \nabla\mu(\mathbf{r}, [\phi(t)]) \quad (12)$$

with the collective diffusion constant D . From the continuity equation of the particle number one obtains the conserved dynamics (model B [24]) equation of motion of $\phi(\mathbf{r}, t)$:

$$\varrho_{\text{max}} \frac{\partial}{\partial t} \phi(\mathbf{r}, t) = -\nabla \cdot \mathbf{j}(\mathbf{r}, [\phi(t)]). \quad (13)$$

In the low-density limit, $\phi(\mathbf{r}, t) \ll 1$, Eqs. (11)–(13) lead to the well-known diffusion equation $\partial\phi(\mathbf{r}, t)/\partial t = D\nabla^2\phi(\mathbf{r}, t)$. However, in general, Eqs. (11)–(13) do *not* correspond to a simple diffusion equation of the occupancy $\phi(\mathbf{r}, t)$ for at least three reasons: First, at higher densities the effective diffusion “constant” becomes $\phi(\mathbf{r}, t)$ -dependent, which renders the problem non-linear. Second, upon deriving an approximate diffusion equation from Eqs. (11)–(13) one has to decide around which reference density to expand, and there is no unique natural choice in the context of liquid-liquid interfaces. Third, the driving force for the diffusion process described by Eqs. (11)–(13) is *not* a non-vanishing gradient in the *density* (consider, e.g., a liquid-liquid interface

at equilibrium), but in the *local chemical potential* (see Eq. (12)). Hence any derivation of a diffusion equation introduces some *assumption* concerning the final structure at the end of the relaxation process. However, Eqs. (11)–(13) lead uniquely, i.e., without further assumptions, from any initial state to that final state which is consistent with the underlying density functional.

In the following a planar surface between liquid and vapor bulk states (see Fig. 1) will be considered. The lateral translational symmetry leads to profiles $\phi(z, t) = \tilde{\phi}(\tilde{z}, \tilde{t})$ which depend only on the coordinate $z = \tilde{z}\lambda$ normal to the surface and on the time $t = \tilde{t}\tau$ with the diffusion time $\tau = \lambda^2/D$. Using Eqs. (1)–(4) one obtains from Eq. (11)

$$\begin{aligned} \tilde{\mu}(\tilde{z}, [\tilde{\phi}]) &:= \frac{\mu(z, [\phi])}{k_B T} \\ &= \ln \left(\frac{\tilde{\phi}(\tilde{z})}{1 - \tilde{\phi}(\tilde{z})} \right) - \frac{3}{2T^*} \int_{-1}^1 du (1 - u^2) \tilde{\phi}(\tilde{z} + u). \end{aligned} \quad (14)$$

Equation (12) leads to

$$\tilde{j}(\tilde{z}, [\tilde{\phi}]) := \frac{j(z, [\phi])}{\varrho_{\max} \lambda / \tau} = -\tilde{\phi}(\tilde{z}) \frac{\partial}{\partial \tilde{z}} \tilde{\mu}(\tilde{z}, [\tilde{\phi}]) \quad (15)$$

and Eq. (13) takes the form

$$\frac{\partial}{\partial \tilde{t}} \tilde{\phi}(\tilde{z}, \tilde{t}) = -\frac{\partial}{\partial \tilde{z}} \tilde{j}(\tilde{z}, [\tilde{\phi}(\tilde{t})]). \quad (16)$$

Equations (14)–(16) demonstrate that, when expressed in terms of the interaction range λ and the diffusion time τ , the temporal evolution of the state of the system $\tilde{\phi}(\tilde{z}, \tilde{t})$ depends only on one parameter: the effective temperature T^* .

In the present study Eqs. (14)–(16) are solved numerically subject to the boundary conditions

$$\tilde{\phi}(\tilde{z} \rightarrow -\infty, \tilde{t} > 0) \rightarrow \phi_L, \quad (17)$$

$$\tilde{\phi}(\tilde{z} \rightarrow +\infty, \tilde{t} > 0) \rightarrow \phi_V, \quad (18)$$

where the bulk occupancies ϕ_L and ϕ_V correspond to the reduced bulk chemical potential differences from coexistence $\Delta\tilde{\mu}_L := \tilde{\mu}_L - \tilde{\mu}_{\text{co}}(T^*) \geq 0$ (liquid) and $\Delta\tilde{\mu}_V := \tilde{\mu}_V - \tilde{\mu}_{\text{co}}(T^*) \leq 0$ (vapor), respectively, at a given temperature $T^* \leq T_c^*$ (see Fig. 1).

Since our interest here is not in describing a realistic system quantitatively but in inferring the general mechanism of interface formation, we consider the artificial but simple initial state

$$\tilde{\phi}(\tilde{z}, \tilde{t} = 0) = \begin{cases} \phi_L & , \tilde{z} < 0 \\ \phi_V & , \tilde{z} \geq 0 \end{cases}. \quad (19)$$

The conclusions to be drawn later are not expected to depend on this choice.

D. Gibbs dividing surface

In order to quantify the amount of colloidal particles evaporating from the liquid into the vapor phase the position of the Gibbs dividing surface $z_{\text{GDS}}(t)$ at time t is introduced by [2]

$$\int_{-\infty}^{z_{\text{GDS}}(t)} dz (\phi(z, t) - \phi_L) + \int_{z_{\text{GDS}}(t)}^{\infty} dz (\phi(z, t) - \phi_V) = 0. \quad (20)$$

In the light of the continuously spreading tails of the liquid-liquid interface to be observed later (see, e.g., Fig. 2(d)) the notion of a Gibbs dividing surface might appear somewhat unusual, but it is only the aspect of the *position* and not that of the (diverging) width which is used here. Taking the derivative of the previous equation with respect to time t leads to

$$\begin{aligned} (\phi_L - \phi_V) \frac{dz_{\text{GDS}}(t)}{dt} &= \int dz \frac{\partial \phi(z, t)}{\partial t} \\ &= -\frac{1}{\varrho_{\max}} \int dz \frac{\partial j(z, t)}{\partial z} \\ &= -\frac{1}{\varrho_{\max}} (j(\infty, t) - j(-\infty, t)) \\ &= 0. \end{aligned} \quad (21)$$

Therefore, the position of the Gibbs dividing surface is independent of time: $z_{\text{GDS}}(t) = z_{\text{GDS}}(0) = 0$ (see Eq. (19)). Consequently, the excess number of particles per cross-sectional area in the liquid phase

$$\Gamma_L(t) := \varrho_{\max} \int_{-\infty}^0 dz (\phi(z, t) - \phi_L) \quad (22)$$

changes with the rate

$$\begin{aligned} \frac{d\Gamma_L(t)}{dt} &= \varrho_{\max} \int_{-\infty}^0 dz \frac{\partial \phi(z, t)}{\partial t} = - \int_{-\infty}^0 dz \frac{\partial j(z, t)}{\partial z} \\ &= -(j(0, t) - j(-\infty, t)) = -j(0, t). \end{aligned} \quad (23)$$

This finding is to be expected due to the underlying conserved dynamics of the colloidal fluid. A dimensionless form of Eq. (22) is given by

$$\tilde{\Gamma}_L(\tilde{t}) := \frac{\Gamma_L(t)}{\varrho_{\max} \lambda} = \int_{-\infty}^0 d\tilde{z} (\tilde{\phi}(\tilde{z}, \tilde{t}) - \phi_L). \quad (24)$$

E. Interfacial tension

The interfacial tension is defined as the work per interfacial area which is required to increase the interfacial

area A but keeping the total volume V as well as the number of particles N constant [2]:

$$\gamma[\phi] = \left(\frac{\partial F[\phi]}{\partial A} \right)_{V,N}. \quad (25)$$

In the present case of a colloidal dispersion a change of the interfacial area between the colloidal liquid and the colloidal vapor could be achieved by deforming the container of the fluid appropriately, which leads to a deformation of the incompressible molecular solvent dragging the dispersed colloids with it. Due to the separation of molecular and colloidal time scales, one is able to perform this deformation, on the one hand, sufficiently slow in order to stay in the regime of low Reynolds numbers

to avoid dissipation due to turbulence, and, on the other hand, sufficiently fast such that the colloidal distribution $\phi(z, t)$ is practically not evolving during the measurement.

Consider the system volume $\mathcal{V} \subseteq \mathbb{R}^3$ and a divergence-free map $\mathbf{w} : \mathcal{V} \rightarrow \mathbb{R}^3$, i.e., $\text{div } \mathbf{w} = 0$, which corresponds to the incompressibility of the solvent. This leads to a shift of any point $\mathbf{r} \in \mathcal{V}$ to the new position $\mathbf{r}_{\mathbf{w}} := \mathbf{r} + \mathbf{w}(\mathbf{r})$ as well as to the deformation of the system volume \mathcal{V} into $\mathcal{V}_{\mathbf{w}} := \{\mathbf{r}_{\mathbf{w}} \in \mathbb{R}^3 | \mathbf{r} \in \mathcal{V}\}$. Moreover, $\text{div } \mathbf{w} = 0$ implies that the number density of colloids does not change due to deformation \mathbf{w} : $\phi_{\mathbf{w}}(\mathbf{r}_{\mathbf{w}}) = \phi(\mathbf{r})$.

The free energy $F_{\mathbf{w}}[\phi_{\mathbf{w}}]$ of the deformed system $\mathcal{V}_{\mathbf{w}}$ in state $\phi_{\mathbf{w}}$ is given by (see Eqs. (2)–(4))

$$\begin{aligned} F_{\mathbf{w}}[\phi_{\mathbf{w}}] &= k_B T \varrho_{\max} \int_{\mathcal{V}_{\mathbf{w}}} d^3 r_{\mathbf{w}} [\phi_{\mathbf{w}}(\mathbf{r}_{\mathbf{w}}) \ln(\phi_{\mathbf{w}}(\mathbf{r}_{\mathbf{w}})) + (1 - \phi_{\mathbf{w}}(\mathbf{r}_{\mathbf{w}})) \ln(1 - \phi_{\mathbf{w}}(\mathbf{r}_{\mathbf{w}}))] \\ &\quad + \frac{\varrho_{\max}^2}{2} \int_{\mathcal{V}_{\mathbf{w}}} d^3 r_{\mathbf{w}} \int_{\mathcal{V}_{\mathbf{w}}} d^3 r'_{\mathbf{w}} U(|\mathbf{r}_{\mathbf{w}} - \mathbf{r}'_{\mathbf{w}}|) \phi_{\mathbf{w}}(\mathbf{r}_{\mathbf{w}}) \phi_{\mathbf{w}}(\mathbf{r}'_{\mathbf{w}}) \\ &= k_B T \varrho_{\max} \int_{\mathcal{V}} d^3 r [\phi(\mathbf{r}) \ln(\phi(\mathbf{r})) + (1 - \phi(\mathbf{r})) \ln(1 - \phi(\mathbf{r}))] \\ &\quad + \frac{\varrho_{\max}^2}{2} \int_{\mathcal{V}} d^3 r \int_{\mathcal{V}} d^3 r' U(|\mathbf{r} - \mathbf{r}' + \mathbf{w}(\mathbf{r}) - \mathbf{w}(\mathbf{r}')|) \phi(\mathbf{r}) \phi(\mathbf{r}'). \end{aligned} \quad (26)$$

Obviously only the RPA part of $F_{\mathbf{w}}[\phi_{\mathbf{w}}]$ depends on the the deformation \mathbf{w} , i.e., only this double volume integral contributes to the interfacial tension Eq. (25).

If the deformation \mathbf{w} stretches the Cartesian z -component $z - z'$ of the difference vector $\mathbf{r} - \mathbf{r}'$ between two points $\mathbf{r}, \mathbf{r}' \in \mathcal{V}$ by a factor η and the projection $\Delta \mathbf{r}_{\perp}$ onto the x - y -plane by, due to $\text{div } \mathbf{w} = 0$, a factor $-\eta/2$, i.e.,

$$\begin{aligned} |\mathbf{r} - \mathbf{r}' + \mathbf{w}(\mathbf{r}) - \mathbf{w}(\mathbf{r}')| \\ = \sqrt{(1 - \eta/2)^2 \Delta r_{\perp}^2 + (1 + \eta)^2 (z - z')^2}, \end{aligned} \quad (27)$$

the RPA part of $F_{\mathbf{w}}[\phi_{\mathbf{w}}]$ equals

$$-\frac{\pi \varepsilon \varrho_{\max}^2 A}{2} \int_{z-\lambda/(1+\eta)}^{z+\lambda/(1+\eta)} dz \phi(z) \int_{z-\lambda/(1+\eta)}^{z+\lambda/(1+\eta)} dz' \frac{\lambda^2 - (1 + \eta)^2 (z - z')^2}{(1 - \eta/2)^2} \phi(z') \quad (28)$$

and the cross-sectional area A is deformed to $A_{\mathbf{w}} = (1 - \eta/2)^2 A$.

Equation (25) leads to

$$\begin{aligned} \gamma[\phi] &= \frac{dF_{\mathbf{w}}[\phi_{\mathbf{w}}]/d\eta}{dA_{\mathbf{w}}/d\eta} \Big|_{\eta=0} \\ &= \frac{\pi \varepsilon \varrho_{\max}^2}{2} \int dz \phi(z) \int_{z-\lambda}^{z+\lambda} dz' (\lambda^2 - 3(z - z')^2) \phi(z') \end{aligned} \quad (29)$$

and with Eq. (6) to

$$\begin{aligned} \tilde{\gamma}[\tilde{\phi}] &:= \frac{\gamma[\phi]}{k_B T \varrho_{\max} \lambda} \\ &= \frac{3}{4T^*} \int_{-1}^1 d\tilde{z} \tilde{\phi}(\tilde{z}) \int_{-1}^1 du (1 - 3u^2) \tilde{\phi}(\tilde{z} + u). \end{aligned} \quad (30)$$

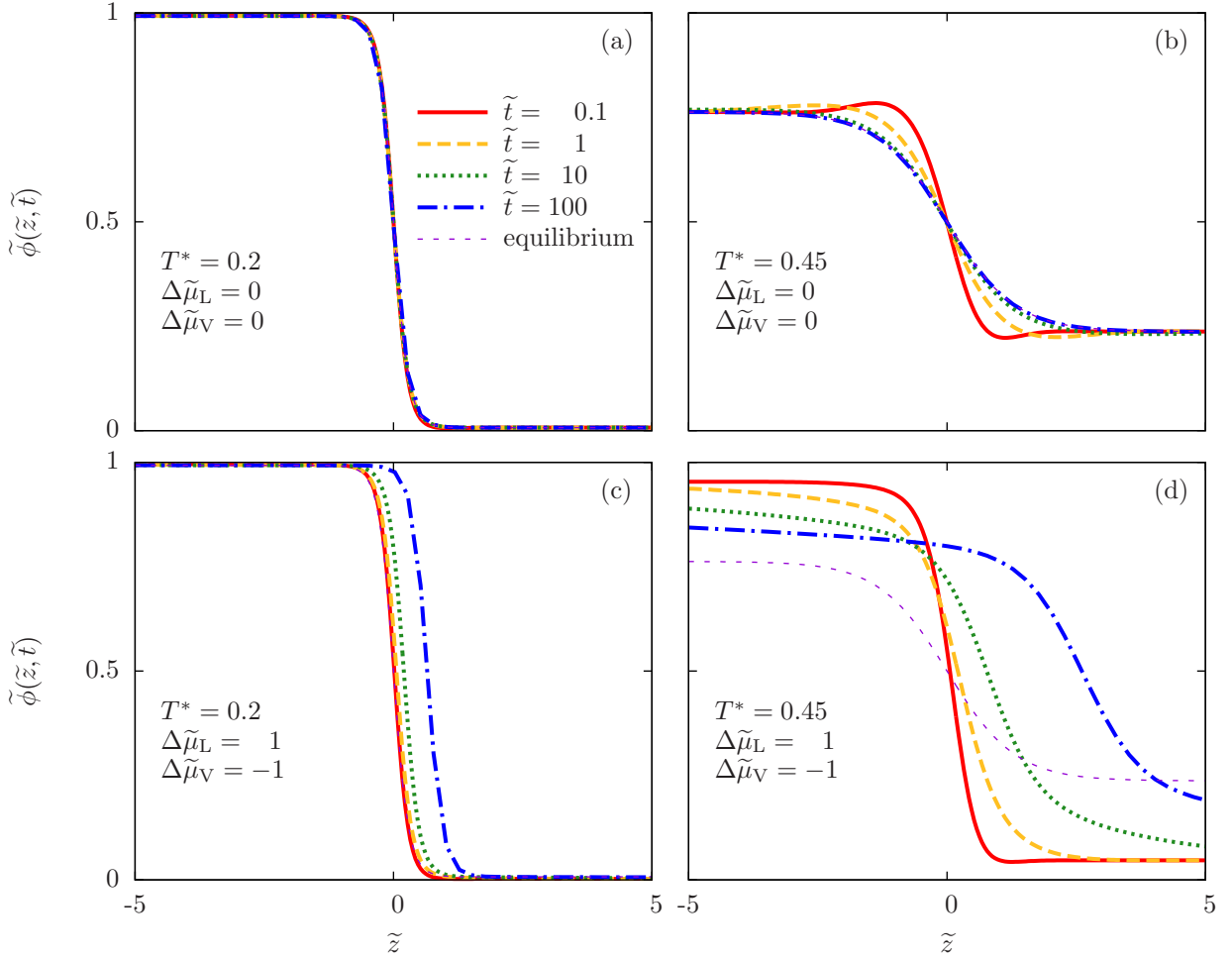


FIG. 2: Temporal evolution of the occupancy profiles $\tilde{\phi}(\tilde{z}, \tilde{t})$ in terms of the dimensionless position $\tilde{z} = z/\lambda$ and the dimensionless time $\tilde{t} = t/\tau$ for reduced temperatures T^* and reduced bulk chemical potential differences from coexistence $\Delta\tilde{\mu}_{L,V}$. Panels (a) and (b) display the relaxation towards the equilibrium interfaces (thin dashed lines) between bulk phases at coexistence, which slows down upon approaching the critical temperature $T_c^* = 1/2$. The symmetry with respect to the critical occupancy $\phi_c = 1/2$ is an irrelevant artifact of the lattice-gas expression Eq. (3). Panels (c) and (d) exemplify the relaxation and translation of the interface in the absence of two-phase coexistence. Far below the critical temperature T_c^* (see panel (c)) the interface relaxation is faster than the translation, whereas the opposite occurs close to the critical point (see panel (d)). For long times during the early-stage relaxation process the structures of the non-equilibrium interfaces become identical to the equilibrium interfaces at the corresponding temperatures T^* .

F. Dissipation rate

The rate of energy dissipation per cross-sectional area is denoted by

$$\begin{aligned} P(t) &= -\frac{dF[\phi(t)]/A}{dt} \\ &= -\frac{1}{A} \int d^3r \frac{\delta F}{\delta \phi(\mathbf{r})}[\phi(t)] \frac{\partial \phi(\mathbf{r}, t)}{\partial t} \\ &= \frac{1}{A} \int d^3r \mu(\mathbf{r}, [\phi(t)]) \nabla \cdot \mathbf{j}(\mathbf{r}, [\phi(t)]). \end{aligned} \quad (31)$$

Since the normal component of the flux \mathbf{j} vanishes at the system boundaries, an integration by parts using the

Gaussian integral theorem leads to

$$\begin{aligned} P(t) &= \frac{1}{A} \int d^3r (-\nabla \mu(\mathbf{r}, [\phi(t)])) \cdot \mathbf{j}(\mathbf{r}, [\phi(t)]) \\ &= \frac{k_B T}{D \varrho_{\max} A} \int d^3r \frac{\mathbf{j}(\mathbf{r}, [\phi(t)])^2}{\phi(\mathbf{r}, t)} \end{aligned} \quad (32)$$

and hence

$$\tilde{P}(\tilde{t}) := \frac{P(t)}{k_B T \varrho_{\max} \lambda / \tau} = \int d\tilde{z} \frac{\tilde{j}(\tilde{z}, [\tilde{\phi}(\tilde{t})])^2}{\tilde{\phi}(\tilde{z}, \tilde{t})}. \quad (33)$$

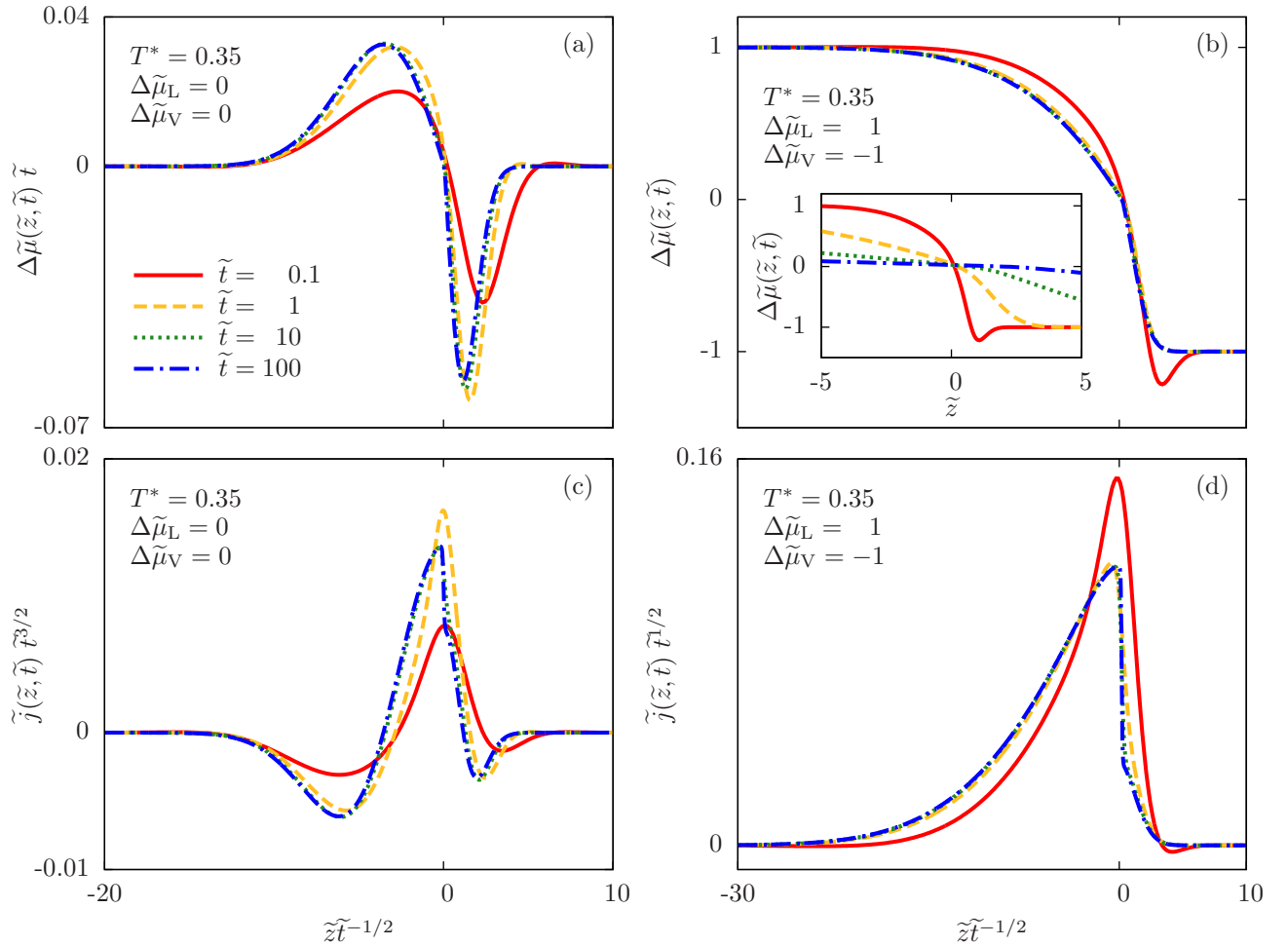


FIG. 3: Scaling behavior of the reduced local chemical potential difference from coexistence $\Delta\tilde{\mu}(\tilde{z}, \tilde{t})$ and of the reduced flux $\tilde{j}(\tilde{z}, \tilde{t})$ in terms of the dimensionless position $\tilde{z} = z/\lambda$ and the dimensionless time $\tilde{t} = t/\tau$ for reduced temperature $T^* = 0.35$. For both bulk phases at coexistence the leading contributions are of the forms $\Delta\tilde{\mu}(\tilde{z}, \tilde{t} \rightarrow \infty) \simeq \tilde{t}^{-1} M_2(\tilde{z}\tilde{t}^{-1/2})$ (panel (a)) and $\tilde{j}(\tilde{z}, \tilde{t} \rightarrow \infty) \simeq \tilde{t}^{-3/2} J_2(\tilde{z}\tilde{t}^{-1/2})$ (panel (c)), whereas in the absence of two-phase coexistence the leading contributions are given by $\Delta\tilde{\mu}(\tilde{z}, \tilde{t} \rightarrow \infty) \simeq M_1(\tilde{z}\tilde{t}^{-1/2})$ (panel (b)) and $\tilde{j}(\tilde{z}, \tilde{t} \rightarrow \infty) \simeq \tilde{t}^{-1/2} J_1(\tilde{z}\tilde{t}^{-1/2})$ (panel (d)). The inset in panel (b) illustrates the temporal increase of the spatial range with $\tilde{\mu}(\tilde{z}, \tilde{t}) \approx \tilde{\mu}_{\text{co}}(T^*)$ around the Gibbs dividing interface at $\tilde{z} = 0$.

III. RESULTS AND DISCUSSION

A. Interfacial structure

Numerical solutions $\tilde{\phi}(\tilde{z}, \tilde{t})$ of Eqs. (14)–(18) are displayed in Fig. 2 for the two representative reduced temperatures $T^* = 0.2$ (panels (a) and (c)) and $T^* = 0.45$ (panels (b) and (d)). The latter temperature is close to the reduced critical temperature $T_c^* = 1/2$, while the former temperature corresponds to a typical triple point temperature, which for many fluids is approximately 40% of the critical temperature [25].

Figures 2(a) and (b) correspond to the relaxation towards the equilibrium interface between both bulk phases at coexistence ($\Delta\tilde{\mu}_L = \Delta\tilde{\mu}_V = 0$). At low reduce temperatures T^* the interface forms rapidly (see Fig. 2(a)), whereas the interface formation is slowed down close to

the critical point (see Fig. 2(b)).

Non-equilibrium conditions are exemplified in Figs. 2(c) and (d) by an oversaturated colloidal liquid ($\Delta\tilde{\mu}_L = 1 > 0$) in contact with an undersaturated colloidal vapor ($\Delta\tilde{\mu}_V = -1 < 0$). Besides the formation of the liquid-vapor interface a drift due to the chemical potential difference between the bulk phases is observed. At low reduce temperatures T^* the interface forms before a significant drift occurs (see Fig. 2(c)), whereas close to the critical point the interface formation is slowed down such that the interface drift sets in before (see Fig. 2(d)).

The remarkable observation to be made in Figs. 2(c) and (d) is that even for strong non-equilibrium conditions ($|\Delta\tilde{\mu}_{L,V}| \ll 1$) the interfacial structures at become identical to that of the equilibrium interfaces (thin dashed lines) at the respective reduced temperature T^* .

In order to understand the formation process of inter-

faces, the reduced local chemical potential difference from coexistence $\Delta\tilde{\mu}(\tilde{z}, \tilde{t}) = \tilde{\mu}(\tilde{z}, \tilde{t}) - \tilde{\mu}_{\text{co}}(T^*)$ and the reduced flux $\tilde{j}(\tilde{z}, \tilde{t})$ are displayed in Fig. 3 for the intermediate reduced temperature $T^* = 0.35$. In the case of both bulk phases being at coexistence ($\Delta\tilde{\mu}_{L,V} = 0$) one infers a scaling behavior $\Delta\tilde{\mu}(\tilde{z}, \tilde{t} \rightarrow \infty) \simeq \tilde{t}^{-1} M_2(\tilde{z}\tilde{t}^{-1/2})$ (Fig. 3(a)) and $\tilde{j}(\tilde{z}, \tilde{t} \rightarrow \infty) \simeq \tilde{t}^{-3/2} J_2(\tilde{z}\tilde{t}^{-1/2})$ (Fig. 3(c)) with scaling functions $M_2(x)$ and $J_2(x)$. However, in the absence of two-phase coexistence $\Delta\tilde{\mu}(\tilde{z}, \tilde{t} \rightarrow \infty) \simeq M_1(\tilde{z}\tilde{t}^{-1/2})$ (Fig. 3(b)) and $\tilde{j}(\tilde{z}, \tilde{t} \rightarrow \infty) \simeq \tilde{t}^{-1/2} J_1(\tilde{z}\tilde{t}^{-1/2})$ (Fig. 3(d)) with scaling functions $M_1(x)$ and $J_1(x)$ is found. The scaling functions $M_{1,2}(x)$ and $J_{1,2}(x)$ in general depend on T^* , $\Delta\tilde{\mu}_L$, and $\Delta\tilde{\mu}_V$. The total scaling behavior may be combined to

$$\Delta\tilde{\mu}(\tilde{z}, \tilde{t} \rightarrow \infty) \simeq M_1(\tilde{z}\tilde{t}^{-1/2}) + \tilde{t}^{-1} M_2(\tilde{z}\tilde{t}^{-1/2}) \quad (34)$$

and

$$\tilde{j}(\tilde{z}, \tilde{t} \rightarrow \infty) \simeq \tilde{t}^{-1/2} J_1(\tilde{z}\tilde{t}^{-1/2}) + \tilde{t}^{-3/2} J_2(\tilde{z}\tilde{t}^{-1/2}). \quad (35)$$

Obviously, Eq. (35) follows from Eq. (34) by means of Eq. (15). For two-phase coexistence the scaling function $M_1(x)$ in Eq. (34) vanishes so that the leading contribution is given by the second term on the right-hand side of Eq. (34). In the absence of two-phase coexistence the scaling function $M_1(x)$ does not vanish identically so that it gives rise to the leading order contribution.

Considering the situation of a non-equilibrium interface displayed in Fig. 3(b), one observes that the reduced local chemical potential $\tilde{\mu}(\tilde{z} \approx 0, \tilde{t})$ in the vicinity of the Gibbs dividing interface is close to the coexistence value $\tilde{\mu}_{\text{co}}(T^*) = -1/T^*$. Then the scaling $\Delta\tilde{\mu}(\tilde{z}, \tilde{t} \rightarrow \infty) \simeq M_1(\tilde{z}\tilde{t}^{-1/2})$ implies $\tilde{\mu}(\tilde{z}, \tilde{t} \rightarrow \infty) \approx \tilde{\mu}_{\text{co}}(T^*)$ for an increasingly wide range $|\tilde{z}| < \tilde{R}(\tilde{t}) \sim \tilde{t}^{1/2}$ around the Gibbs dividing interface (see inset in Fig. 3(b)). Once $\tilde{R}(\tilde{t})$ exceeds the bulk correlation length, the local chemical potential in the interfacial range coincides with that of the equilibrium interface. Therefore, for during the early-stage relaxation process non-equilibrium interfaces approach the same structure as the equilibrium interface at the same temperature, because the finite chemical potential difference between the bulk phases is bridged by the local chemical potential over an unlimited spatial range so that locally, at the interface position, an effectively uniform chemical potential profile is sensed by the fluid.

B. Interfacial tension

The phenomenon of non-equilibrium interfaces to approach the structure of equilibrium interfaces discussed in the previous Subsec. III A implies the approach of the interfacial tension Eq. (30) towards the equilibrium value. This expectation is confirmed in Fig. 4, which displays the interfacial tension $\tilde{\gamma}(\tilde{t}) = \tilde{\gamma}[\tilde{\phi}(\tilde{t})]$ as a function of the dimensionless time \tilde{t} for various equilibrium and non-equilibrium conditions of the bulk phases and

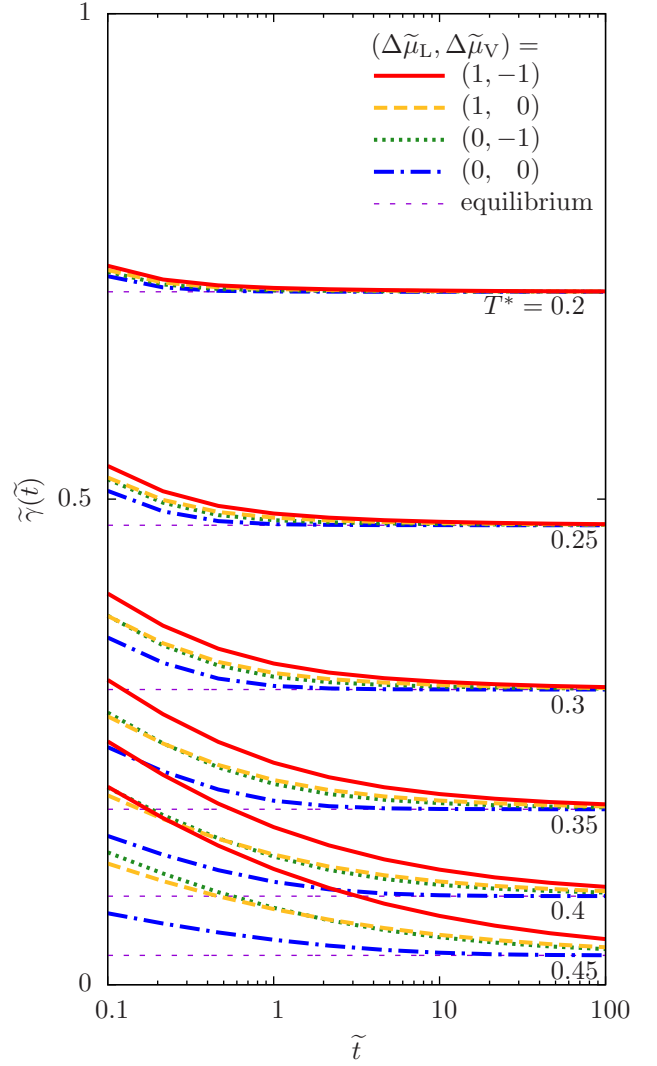


FIG. 4: Temporal evolution of the reduced interfacial tension $\tilde{\gamma}(\tilde{t})$ in terms of the dimensionless time $\tilde{t} = t/\tau$ for various reduced temperatures T^* . Irrespective of the states $\Delta\tilde{\mu}_{L,V}$ of the bulk phases, the interfacial tension approaches the values of the equilibrium interfaces (thin horizontal dashed lines) at the respective reduced temperatures T^* .

several reduced temperatures T^* . The curves approach the equilibrium values (thin horizontal dashed lines) at the respective temperatures. As is intuitively expected the initial deviations of the interfacial tension from its equilibrium value increase with the deviations of the two bulk fluids from two-phase coexistence. Consequently the larger the deviation from two-phase coexistence is, the longer the relaxation of the interfacial tension to its final equilibrium value takes.

The actual mode of relaxation towards the equilibrium value of the interfacial tension can be inferred from Fig. 5, which displays the difference $\Delta\tilde{\gamma}(\tilde{t})$ of the interfacial tension at dimensionless time \tilde{t} from the final equilibrium value for the reduced temperature $T^* = 0.35$. It can be observed that for two-phase coexistence the relaxation

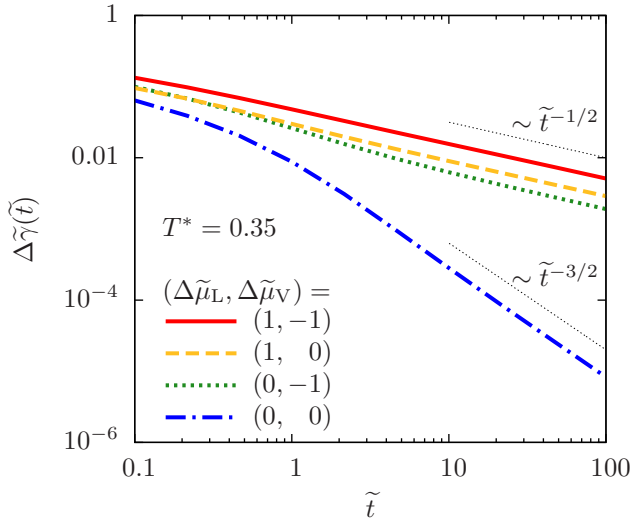


FIG. 5: Deviation $\Delta\tilde{\gamma}(\tilde{t})$ of the interfacial tension from the equilibrium value as a function of the dimensionless time $\tilde{t} = t/\tau$ for reduced temperature $T^* = 0.35$. As a function of time \tilde{t} the relaxation occurs algebraically according to $\Delta\tilde{\gamma}(\tilde{t} \rightarrow \infty) \sim \tilde{t}^{-3/2}$ for both bulk phases at coexistence and $\Delta\tilde{\gamma}(\tilde{t} \rightarrow \infty) \sim \tilde{t}^{-1/2}$ for non-equilibrium conditions.

occurs according to $\Delta\tilde{\gamma}(\tilde{t}) \sim \tilde{t}^{-3/2}$, whereas in the absence of two-phase coexistence the decay is of the form $\Delta\tilde{\gamma}(\tilde{t}) \sim \tilde{t}^{-1/2}$. The algebraic relaxation of the interfacial tension is related to the underlying conserved dynamics, which requires rearrangements of the fluid to occur by transport. The observation that the relaxation in the case of two-phase coexistence is faster (with exponent $-3/2$) than in the absence of two-phase coexistence (with exponent $-1/2$) can be understood by noting that in the former situation only the interface relaxes, whereas in the latter situation the interface relaxation occurs on top of a diffusive flow from one bulk phase to the other.

C. Energy dissipation

During the formation of the interface or the evaporation of particles from the oversaturated into the undersaturated bulk phase energy is dissipated, which corresponds to a decrease of the total Helmholtz free energy $F[\phi(t)]$. Since an isothermal system is considered here the dissipated energy is absorbed by the heat bath. Figure 6 displays the reduced energy dissipation rate $\tilde{P}(\tilde{t})$ defined in Eq. (33) for reduced temperature $T^* = 0.35$ and various equilibrium and non-equilibrium conditions. The dissipation rate decays algebraically according to $\tilde{P}(\tilde{t} \rightarrow \infty) \sim \tilde{t}^{-5/2}$ for two-phase coexistence and $\tilde{P}(\tilde{t} \rightarrow \infty) \sim \tilde{t}^{-1/2}$ otherwise. These exponents are a simple consequence of Eq. (35) used in Eq. (33).

The origin of the observed differences between the case of two-phase coexistence and that of non-equilibrium conditions is again the fact that in the absence of two-phase

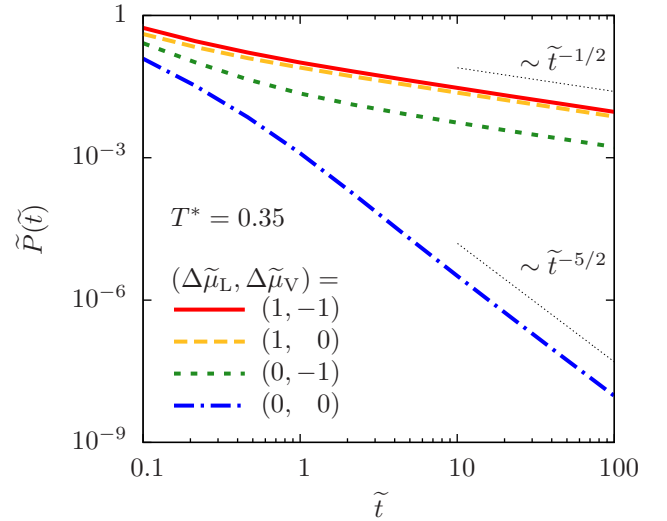


FIG. 6: Reduced energy dissipation rate $\tilde{P}(\tilde{t})$ per cross-sectional area as a function of the dimensionless time $\tilde{t} = t/\tau$ for reduced temperature $T^* = 0.35$. As a function of time \tilde{t} the dissipation decays algebraically according to $\tilde{P}(\tilde{t} \rightarrow \infty) \sim \tilde{t}^{-5/2}$ for both bulk phases at coexistence and $\tilde{P}(\tilde{t} \rightarrow \infty) \sim \tilde{t}^{-1/2}$ for non-equilibrium conditions.

coexistence dissipation is dominated by the diffusive flow induced by the two bulk phases being not at equilibrium with each other, which does not occur for two-phase coexistence.

D. Evaporation

In the absence of two-phase coexistence with an oversaturated liquid and/or an undersaturated vapor phase one expects evaporation of the liquid. This terminology is used here also in the context of colloidal fluids with colloid-rich (liquid) and colloid-poor (vapor) phases. Amongst the various possibilities to quantify evaporation two are shown in Fig. 7.

Figure 7(a) displays the reduced number of evaporated particles per cross-sectional area $-\tilde{\Gamma}_L(\tilde{t})$, which is identical to the negative of the reduced excess number of particles per cross-sectional area in the liquid (see Eq. (24)). The asymptotic behavior is given by $-\tilde{\Gamma}_L(\tilde{t} \rightarrow \infty) \sim \tilde{t}^{1/2}$. Therefore, the number of evaporated particles is not bounded, but the rate of evaporation is approaching zero.

Figure 7(b) depicts the absolute reduced interface position $|\tilde{z}_{1/2}(\tilde{t})|$, which is defined by the location of the occupancy 50%, i.e., by $\tilde{\phi}(\tilde{z}_{1/2}(\tilde{t}), \tilde{t}) = 1/2$. One observes $|\tilde{z}_{1/2}(\tilde{t} \rightarrow \infty)| \sim \tilde{t}^{1/2}$, which implies that the interface is shifted infinitely far from the location of the Gibbs dividing interface. It is interesting to note that $\tilde{z}_{1/2}(\tilde{t})$ is positive, i.e., the interface is shifted towards the vapor phase, for $(\Delta\tilde{\mu}_L, \Delta\tilde{\mu}_V) = (1, -1)$ and $(1, 0)$, whereas it is negative, i.e., the interface is shifted towards the liquid phase, for $(\Delta\tilde{\mu}_L, \Delta\tilde{\mu}_V) = (0, -1)$. This finding may

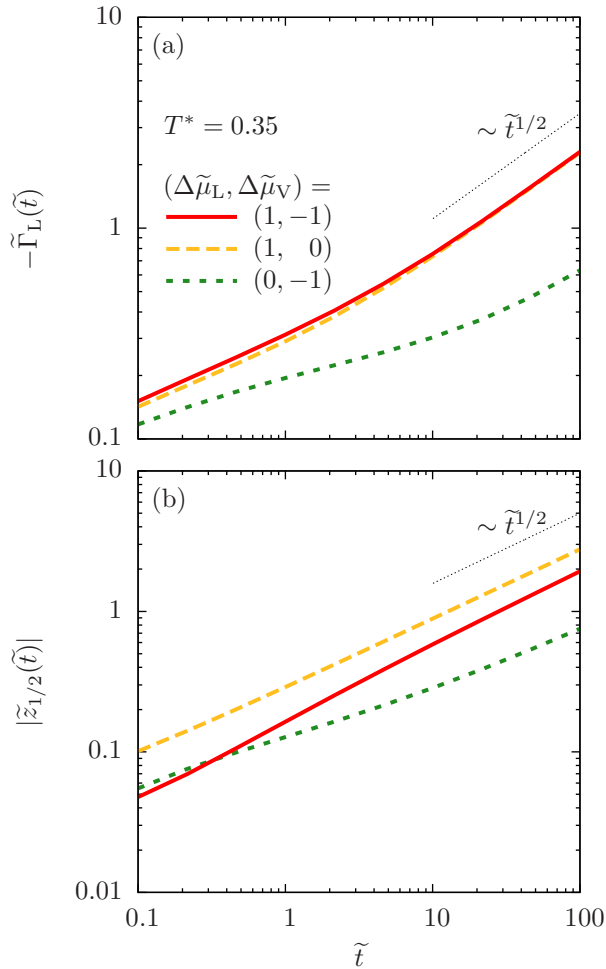


FIG. 7: Reduced number of evaporated particles $-\tilde{\Gamma}_L(\tilde{t})$ per cross-sectional area (panel (a)) and absolute reduced interface position $|\tilde{z}_{1/2}(\tilde{t})|$, where $\tilde{\phi}(\tilde{z}_{1/2}(\tilde{t}), \tilde{t}) = 1/2$, (panel (b)) as functions of the reduced time $\tilde{t} = t/\tau$ for reduced temperature $T^* = 0.35$. Both quantities increase algebraically $\sim \tilde{t}^{1/2}$.

be illustrated by saying that an oversaturated liquid is “flooding” the vapor phase, whereas an undersaturated vapor is “eroding” the liquid phase.

IV. CONCLUSIONS AND SUMMARY

In this work the early-stage relaxation of equilibrium and non-equilibrium interfaces in colloidal dispersions have been studied, which can separate in a colloidal-rich (liquid) phase and a colloidal-poor (vapor) phase (Fig. 1). Close to the critical point the interface formation is considerably slowed down as compared to temperatures further away (Fig. 2). Moreover, for the bulk phases being not at equilibrium the process of interface formation is superimposed by the evaporation of colloidal particles from the liquid into the vapor phase (Fig. 2). However, the most surprising observation is that, irrespective of how much the bulk phases differ from two-phase coexis-

tence, the interfacial structure approaches that at two-phase coexistence during the early-stage relaxation process. This surprising observation implies that the relaxation towards global equilibrium of the interface is not following but preceding that of the bulk phases, i.e., the interface relaxes independently of the bulk phases.

During the early-stage relaxation process the local chemical potential and the flux, which, as functions of position, interpolate between the corresponding bulk values, approach scaling forms (Fig. 3 and Eqs. (34) and (35)). On the one hand, the leading order contributions in this scaling exhibit power-law behavior in time, the values of the exponents of which depend on whether an equilibrium or a non-equilibrium system is considered (Eqs. (34) and (35)). The occurrence of power-law behavior is linked to the underlying conserved dynamics (model B), while a non-conserved dynamics (e.g., model A [24]) would give rise to an exponential decay. On the other hand, the spatial range in which the local chemical potential interpolates between the bulk values grows diffusively with time so that the gradient, and thus the flux, decays with time. Hence, the chemical potential becomes locally constant during the early-stage relaxation process, which, at the value of the coexistence chemical potential, explains the occurrence of a liquid-vapor interfacial structure identical to that for two-phase coexistence, even in non-equilibrium systems. Consequently, the interfacial tension decays to the value at two-phase coexistence irrespective of whether an equilibrium or a non-equilibrium system is considered (Fig. 4), while the degree of non-equilibrium merely determines the quantitative deviation from the equilibrium value.

Concerning the questions raised in the Introduction on non-equilibrium interfaces in molecular fluids one notes that these systems, in contrast to colloidal fluids, have to be described by model H dynamics [24] rather than by model B dynamics. Hence, due to the possibility of waves and turbulence within model H dynamics, it is conceivable that the decay modes of the interfacial tensions (Fig. 5) and of the dissipation rates (Fig. 6) could be different for molecular and for colloidal fluids. However, due to the line of arguments for model B dynamics given above, which merely relies on the existence of a local chemical potential which interpolates between the bulk values and which becomes locally constant, the interfacial tensions in non-equilibrium systems within model H dynamics can also be expected to approach the coexistence values during the early-stage relaxation process.

Finally, the evaporation of colloidal particles from the liquid into the vapor phase in non-equilibrium systems exhibits diffusive signatures (Fig. 7), which is obviously linked to the underlying conserved dynamics.

To summarize the present work, the early-stage relaxation of an interface in non-equilibrium colloidal fluids, during which the interface but not the bulk phases relax, towards that for two-phase coexistence has been observed, explained and quantified within a simple model. It has been argued that during the early-stage process

an approach of quantities such as the interfacial tension towards the equilibrium values can be expected to occur also for molecular fluids, whose dynamics differ from that of colloidal fluids. Experimental investigations using colloidal fluids may be interesting to verify the theoretical picture obtained here.

Acknowledgments

We like to thank S. Dietrich, R. Evans, M. Krüger, A. Maciolek and P. Teixeira for helpful comments.

-
- [1] S. Dietrich, in *Phase transitions and critical phenomena*, Vol. 12, edited by C. Domb and J.L. Lebowitz (Academic, London, 1988), p. 1.
 - [2] J.S. Rowlinson and B. Widom, *Molecular theory of capillarity* (Dover, Mineola, 2002).
 - [3] J. Drelich, Ch. Fang, and C.L. White, *Interfacial Tension Measurement in Fluid-Fluid Systems*, in *Encyclopedia of Surface and Colloid Science*, Vol. 4, edited by P. Somasundaran (Taylor & Francis, New York, 2006), p. 2966.
 - [4] R. Millner, P. Joos, and V.B. Fainerman, *Adv. Colloid Interface Sci.* **49**, 249 (1994).
 - [5] J. Eastoe and J.S. Dalton, *Adv. Colloid Interface Sci.* **85**, 103 (2000).
 - [6] R. Defay, I. Prigogine, and A. Sanfeld, *J. Colloid Interface Sci.* **58**, 498 (1977).
 - [7] R.F. Kayser, M.R. Moldover, and J.W. Schmidt, *J. Chem. Soc., Faraday Trans. 2* **82**, 1701 (1986).
 - [8] R. Lipowsky and D.A. Huse, *Phys. Rev. Lett.* **57**, 353 (1986).
 - [9] S. Peach and C. Franck, *J. Chem. Phys.* **104**, 686 (1996).
 - [10] A.V. Lukyanov and A.E. Likhtman, *J. Chem. Phys.* **138**, 034712 (2013).
 - [11] D.G.A.L. Aarts, H.N.W. Lekkerkerker, *J. Phys.: Condens. Matter* **16**, S4231 (2004).
 - [12] D.G.A.L. Aarts, M. Schmidt, H.N.W. Lekkerkerker, *Science* **304**, 847 (2004).
 - [13] K. Kawasaki, *Physica A* **208**, 35 (1994).
 - [14] D. Dean, *J. Phys. A* **29**, L613 (1996).
 - [15] U. Marini Bettolo Marconi and P. Tarazona, *J. Chem. Phys.* **110**, 8032 (1999).
 - [16] U. Marini Bettolo Marconi and P. Tarazona, *J. Phys.: Condens. Matter* **12**, A413 (2000).
 - [17] R. Evans, *Adv. Phys.* **28**, 143 (1979).
 - [18] W. Dieterich, H.L. Frisch, and A. Majhofer, *Z. Phys. B* **78**, 317 (1990).
 - [19] C. Ebner, W.F. Saam, and D. Stroud, *Phys. Rev. A* **14**, 2264 (1976).
 - [20] Y. Rosenfeld, *Phys. Rev. Lett.* **63**, 980 (1989).
 - [21] R. Roth, R. Evans, A. Lang, and G. Kahl, *J. Phys.: Condens. Matter* **14**, 12063 (2002).
 - [22] H. Hansen-Goos and K. Mecke, *Phys. Rev. Lett.* **102**, 018302 (2009).
 - [23] D.G.A.L. Aarts, *J. Phys. Chem. B* **109**, 7407 (2005).
 - [24] P.C. Hohenberg and B.I. Halperin, *Rev. Mod. Phys.* **49**, 435 (1977).
 - [25] D.R. Lide (ed.), *CRC Handbook of Chemistry and Physics*, (CRC Press, Boca Raton, 1998)